$$\sum_{M_c \mu m} (J_{cs} l J M \mid J_c M_c, s\mu, lm) \times (J_c M_c, s\mu, lm \mid J'_{cs} l J' M) = \delta_{J_{cs} J'_{cs}} \delta_{JJ'}.$$

[14]In this regard see the first two paragraphs of Ref. 9, Sec. I.

[15]P. M. Mitchell and K. Codling, Phys. Letters 38A, 31 (1972).

[16]M. J. Van der Wiel and C. E. Brion, J. Electr. Spectrosc. 1, 739 (1973).

[17]The photoionization spectrum of Hg below the $Hg^+$ ($^2D_{5/2}$) threshold has been studied by several authors: (a) B. Brehm, Z. Naturforsch. 21a, 196 (1966); (b) J. Berkowitz and C. Lifshitz, J. Phys. B 1, 438 (1968); (c) R. B. Cairns, H. Harrison, and R. I. Schoen, J. Chem. Phys. 53, 96 (1970).

[18]Depolarization of angular correlations, owing to the lack of information about the orientation of unobserved angular momenta, is a concept that is central to the theory of angular correlation. See U. Fano and G. Racah, *Irreducible Tensorial Sets* (Academic, New York, 1959), Chap. 19, and especially p. 110, last paragraph.

[19]W. C. Martin, J. Sugar, and J. L. Tech, Phys. Rev. A 6, 2022 (1972) have verified the triplet character of this level using intermediate coupling theory with configuration interaction. They report that the $5d^9(^2D_{3/2})\,6s^2 6p_{3/2}$ ($J=1$, $\pi=-1$) level at 11.62 eV is composed of 63.3% $^3D_1^\circ$, and 29.5% $^3P_1^\circ$, the total singlet composition is less than 7%. These authors find substantial triplet character for many of the autoionizing levels of Hg [see also W. C. Martin, J. Sugar, and J. L. Tech, J. Opt. Soc. Am. 62, 1488 (1972)]. The deviation of $\beta$ from 2 is evidence of this triplet character.

PHYSICAL REVIEW A VOLUME 7, NUMBER 6 JUNE 1973

# Variational Calculations of Electron–Alkali-Metal-Atom Scattering: Elastic Scattering by Li, Na, and K†

A.-L. Sinfailam* and R. K. Nesbet
*IBM Research Laboratory, San Jose, California 95193*
(Received 14 February 1973)

Elastic total and spin-exchange cross sections are computed for electron scattering by Li, Na, and K, for energies below the first excitation threshold. The method used is the variational form of solution of continuum Bethe-Goldstone equations. Results are in substantial agreement with close-coupling calculations and with recent experimental data.

## I. INTRODUCTION

This paper presents results of variational calculations of electron scattering by Li, Na, and K atoms in the low-energy region, below the $n_0p$ excitation threshold for atomic ground-state configurations $n_0s$. The method has been described in sufficient detail elsewhere,[1] and will not be repeated here. Variational equations are solved equivalent to the continuum Bethe–Goldstone equation for the incident and series electrons in electron–alkali-metal-atom scattering.[2] The method is similar to that of Harris and Michels.[3] The specific variational formalism used here is the "optimized anomaly-free" (OAF) method.[4]

Detailed close-coupling calculations of low-energy-electron scattering by alkali-metal atoms have recently been published.[5,6] The present results, using quite different methodology, essentially confirm these close-coupling results, while providing a test of the new methods used here. Only the lowest-order phase shifts have been computed ($L=0$, 1, 2 for singlet and triplet states). The results obtained indicate that in the elastic scattering region higher-order phase shifts would simply duplicate results already obtained by close-coupling calculations or by the polarization formula used by Moores and Norcross for $L \geq 8$.

Theoretical and experimental results on electron–alkali-metal elastic scattering have been reviewed by Bederson.[7] Recent literature is discussed by Moores and Norcross.[6]

## II. CHOICE OF BASIS FUNCTIONS

In a previous publication[1] we have described an investigation of the relative convergence properties of two methods of choosing basis functions for linear expansion of the variational wave function. Radial orbital basis functions are of the form

$$\phi_i = N r^{n-1} e^{-\zeta r} Y_{\ell m}(\theta, \phi)\ . \qquad (1)$$

With the $e^- + He$ problem as a test case, two methods of choosing basis functions were examined: (i) a sequence of exponents $\zeta$ in *decreasing* geometric progression for fixed $n$, complemented by an increasing arithmetic sequence of exponents for the same index $n$, (ii) a sequence of exponents $\zeta$ in *increasing* geometric progression for fixed $n$, complemented by a sequence with fixed $\zeta$ and increasing powers $n$. It can be shown that both methods

define complete basis sets as the number of functions increases without limit. The calculations on $e^-$ + He indicate that method (i) gives more consistent results.[1] This method has been adopted for the present calculations.

States of the target alkali atoms are taken into account by adding orbitals describing the ground state to set (i) or (ii). The target-atom basis orbitals are those of Nesbet[8] for Li, and the double-$\zeta$ functions of Clementi[9] for Na and K, except that inner-shell orbitals are represented by a single exponent.[10] Preliminary calculations on $e^-$ + Li indicate that results using the target functions of Nesbet,[8] Clementi,[9] and Weiss[11] are similar. This is partly due to the fact that in the present work all basis orbitals are used in the expansion of each variational orbital, whether the latter is identified with the target atom, with the external orbital of a closed channel, or with a perturbation of an external open-channel orbital. Inadequacies in the target-atom basis are compensated by functions from sequences (i) or (ii). A double-$\zeta$ representation of the $n_0p$ excited valence orbital is included in each basis set.

Exponents defining the orbital basis sets used here are listed in Table I.

## III. RESULTS

### A. Phase Shifts

Calculations have been made on the elastic scattering of electrons by Li, Na, and K for $s$-, $p$-, and $d$-orbital waves. Polarization and correlation effects are taken into account by the inclusion of the virtual excitation of the outermost $n_0s$ electron from the ground state of the target atom, using the Bethe–Goldstone method.[2] In this way, we include not only the excited state $n_0p$ of the target, which contributes most of the dominant dipole polarizability of the $n_0s$ state, but also all higher-order singly excited states that can be constructed from the given set of basis orbitals.

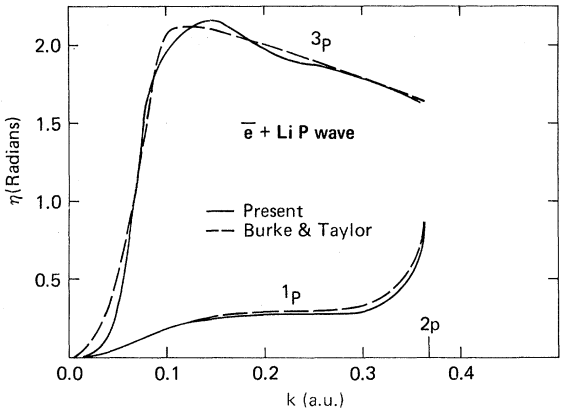


FIG. 2. $L=1$ singlet and triplet phase shifts for scattering by Li.

In Table II we present the results of the calculations. In Fig. 1 we compare our $s$-wave results for Li with previous calculations. Our $^3S$ results agree well with those of Norcross,[6] who has used a scaled Thomas–Fermi statistical model potential modified by a term allowing core polarization. The two-state close-coupling calculation of Burke and Taylor[12] shows a sharp peak at low energy; this is due to a breakdown of the asymptotic expansion of Burke and Schey[13] for very small energies.[6] Our work shows a small peak in the phase shift in the energy range $k \to 0$, in agreement with the calculation of Norcross. Our $^1S$ results agree exactly with those of Norcross; there is also good agreement with Burke and Taylor except at thermal energies, where their calculation is apparently incorrect for the reason given above.

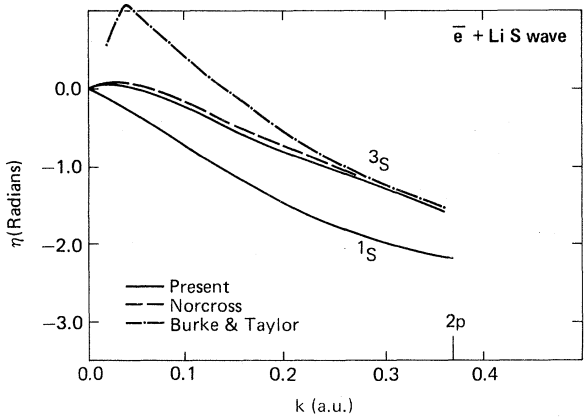


FIG. 1. $L=0$ singlet and triplet phase shifts for scattering by Li.

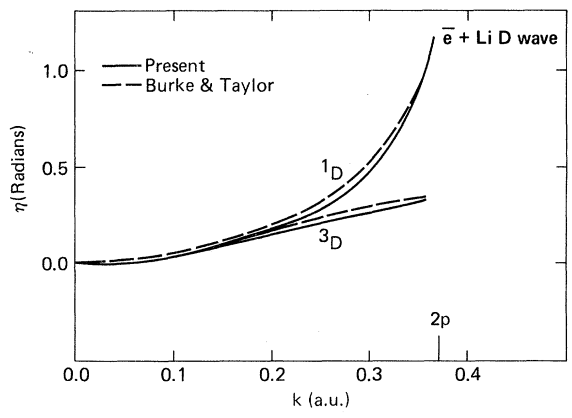


FIG. 3. $L=2$ singlet and triplet phase shifts for scattering by Li.

TABLE I. Orbital basis sets.

| | | |
|---|---|---|
| | | $e^-$ + Li |
| $s$ wave | $s$ | $n=1$, $\zeta=2.6906, 1.0, 0.5, 0.25, 0.125, 0.0625, 0.03125, 2.0$ |
| | | $n=2$, $\zeta=0.6714, 1.9781$ |
| | $p$ | $n=2$, $\zeta=0.6024, 0.4859, 2.0, 1.0, 0.25, 0.125, 0.0625, 4.0$ |
| $p$ wave | $s$ | $n=1$, $\zeta=2.6906, 1.0, 0.5, 0.25, 0.125, 0.0625$ |
| | | $n=2$, $\zeta=0.6714, 1.9781$ |
| | $p$ | $n=2$, $\zeta=0.6024, 0.4859, 2.0, 1.0, 0.25, 0.125, 0.0625$ |
| | $d$ | $n=3$, $\zeta=3.0, 1.5, 0.75, 0.375, 0.1875, 5.0$ |
| $d$ wave | $s$ | $n=1$, $\zeta=2.6906$ |
| | | $n=2$, $\zeta=0.6714, 1.9781$ |
| | $p$ | $n=2$, $\zeta=0.6024, 0.4859, 1.0, 0.25, 0.125$ |
| | $d$ | $n=3$, $\zeta=1.5, 0.75, 0.375, 0.1875$ |
| | $f$ | $n=4$, $\zeta=2.0, 1.0, 0.5, 0.25$ |
| | | $e^-$ + Na |
| $s$ wave | $s$ | $n=1$, $\zeta=10.6259$ |
| | | $n=2$, $\zeta=3.2857$ |
| | | $n=3$, $\zeta=0.7549, 1.2594, 0.3, 0.09, 3.0, 5.0$ |
| | $p$ | $n=2$, $\zeta=3.4009$ |
| | | $n=3$, $\zeta=0.7549, 1.2594, 0.3, 0.09, 3.0, 5.0$ |
| $p$ wave | $s$ | $n=1$, $\zeta=10.6259$ |
| | | $n=2$, $\zeta=3.2857$ |
| | | $n=3$, $\zeta=0.7549, 1.2594, 0.3, 0.09, 2.0, 3.0$ |
| | $p$ | $n=2$, $\zeta=3.4009$ |
| | | $n=3$, $\zeta=0.7549, 1.2594, 0.3, 0.09, 2.0, 3.0$ |
| | $d$ | $n=3$, $\zeta=0.3, 0.09, 0.6, 1.0, 2.0, 3.0$ |
| $d$ wave | $s$ | $n=1$, $\zeta=10.6259$ |
| | | $n=2$, $\zeta=3.2857$ |
| | | $n=3$, $\zeta=0.7549, 1.2594$ |
| | $p$ | $n=2$, $\zeta=3.4009$ |
| | | $n=3$, $\zeta=0.7549, 1.2594, 0.3, 0.09, 2.5$ |
| | $d$ | $n=3$, $\zeta=1.0, 0.6, 0.3, 0.09, 2.5$ |
| | $f$ | $n=4$, $\zeta=1.333, 0.8, 0.4, 0.12, 2.5$ |
| | | $e^-$ + K |
| $s$ wave | $s$ | $n=1$, $\zeta=18.4895$ |
| | | $n=2$, $\zeta=6.5031$ |
| | | $n=3$, $\zeta=2.8933$ |
| | | $n=4$, $\zeta=0.8738, 0.3, 0.09, 0.027, 0.0081, 1.5$ |
| | $p$ | $n=2$, $\zeta=7.5136$ |
| | | $n=3$, $\zeta=2.5752$ |
| | | $n=4$, $\zeta=0.8738, 0.3, 0.09, 0.027, 0.0081, 1.5$ |
| $p$ wave | $s$ | $n=1$, $\zeta=18.4895, 1.0, 0.3, 0.09, 0.027, 0.0081, 2.0$ |
| | | $n=2$, $\zeta=6.5031$ |
| | | $n=3$, $\zeta=2.8933$ |
| | | $n=4$, $\zeta=0.8738$ |
| | $p$ | $n=2$, $\zeta=7.5136, 2.0, 0.6, 0.18, 0.054, 0.0162, 1.0$ |
| | | $n=3$, $\zeta=2.5752$ |
| | | $n=4$, $\zeta=0.8738$ |
| | $d$ | $n=3$, $\zeta=3.0, 0.9, 0.27, 0.081, 0.0243, 2.0, 5.0$ |
| $d$ wave | $s$ | $n=1$, $\zeta=18.4895$ |
| | | $n=2$, $\zeta=6.5031$ |
| | | $n=3$, $\zeta=2.8933$ |
| | | $n=4$, $\zeta=0.8738$ |
| | $p$ | $n=2$, $\zeta=7.5136$ |
| | | $n=3$, $\zeta=2.5752$ |
| | | $n=4$, $\zeta=0.8738, 0.3, 0.09, 1.5, 3.5$ |
| | $d$ | $n=3$, $\zeta=0.75$ |
| | | $n=4$, $\zeta=0.6, 0.3, 0.09, 1.5, 3.5$ |
| | $f$ | $n=4$, $\zeta=1.0, 0.6, 0.3, 0.09, 1.5, 3.5$ |

TABLE II. Scattering phase shifts (rad).

| $k$ (a.u.) | (eV) | $^1S$ | $^3S$ | $^1P$ | $^3P$ | $^1D$ | $^3D$ |
|---|---|---|---|---|---|---|---|
| | | | $e^- - Li$ | | | | |
| 0.05 | 0.034 | −0.343 | 0.017 | 0.058 | 0.307 | 0.003 | 0.003 |
| 0.10 | 0.136 | −0.773 | −0.234 | 0.189 | 1.952 | 0.038 | 0.037 |
| 0.15 | 0.306 | −1.145 | −0.505 | 0.239 | 2.162 | 0.099 | 0.093 |
| 0.20 | 0.544 | −1.490 | −0.788 | 0.272 | 1.981 | 0.175 | 0.151 |
| 0.25 | 0.850 | −1.751 | −1.049 | 0.279 | 1.876 | 0.277 | 0.202 |
| 0.30 | 1.224 | −1.977 | −1.280 | 0.301 | 1.787 | 0.473 | 0.264 |
| 0.35 | 1.667 | −2.144 | −1.515 | 0.525 | 1.660 | 0.892 | 0.322 |
| | | | $e^- - Na$ | | | | |
| 0.05 | 0.034 | −0.410 | −0.047 | 0.087 | 0.230 | 0.010 | 0.010 |
| 0.10 | 0.136 | −0.946 | −0.310 | 0.176 | 1.315 | 0.042 | 0.041 |
| 0.15 | 0.306 | −1.284 | −0.598 | 0.266 | 1.774 | 0.081 | 0.071 |
| 0.20 | 0.544 | −1.610 | −0.883 | 0.254 | 1.717 | 0.181 | 0.147 |
| 0.25 | 0.850 | −1.894 | −1.153 | 0.251 | 1.627 | 0.315 | 0.233 |
| 0.30 | 1.224 | −2.128 | −1.417 | 0.242 | 1.489 | 0.507 | 0.308 |
| 0.35 | 1.667 | −2.305 | −1.669 | 0.374 | 1.388 | 0.572 | 0.291 |
| | | | $e^- - K$ | | | | |
| 0.05 | 0.034 | −0.567 | −0.065 | 0.150 | 2.706 | 0.024 | 0.024 |
| 0.10 | 0.136 | −1.227 | −0.427 | 0.315 | 2.348 | 0.068 | 0.061 |
| 0.15 | 0.306 | −1.573 | −0.800 | 0.383 | 2.022 | 0.218 | 0.169 |
| 0.20 | 0.544 | −1.890 | −1.112 | 0.331 | 1.788 | 0.437 | 0.309 |
| 0.25 | 0.850 | −2.166 | −1.428 | 0.260 | 1.443 | 0.679 | 0.433 |
| 0.30 | 1.224 | −2.400 | −1.744 | 0.353 | 1.290 | 1.003 | 0.440 |

Figures 2 and 3 show, respectively, the $P$ and $D$ results for Li. The $^3P$ phase shift indicates the existence of a narrow resonance above the $2s$ threshold, while the $^1P$ phase shift increases rapidly near the $2p$ threshold. This can be considered to be a resonance enhancing a threshold cusp effect.[14] The rapid increase in the $^1D$ phase shift indicates the existence of a resonance in this channel near the $2p$ threshold.

The results for the $s$, $p$, and $d$ waves for Na are shown in Figs. 4–6. Our work shows good agreement with the Thomas–Fermi calculation of Norcross,[6] and also with the close-coupling calculations of Moores and Norcross, who obtained essentially the same results using two, three, and four states.[6] The results for Na show all the essential features mentioned above for scattering by Li; i.e., (a) small peak in the $^3S$ phase shift for

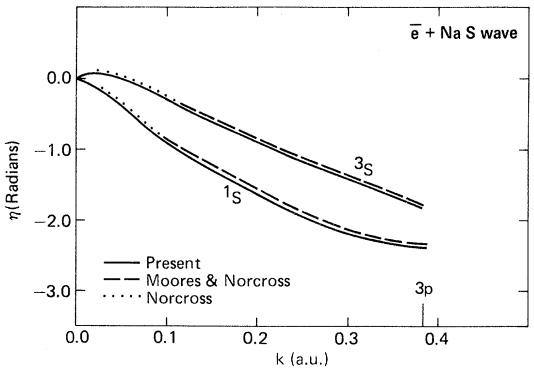


FIG. 4. $L=0$ singlet and triplet phase shifts for scattering by Na.

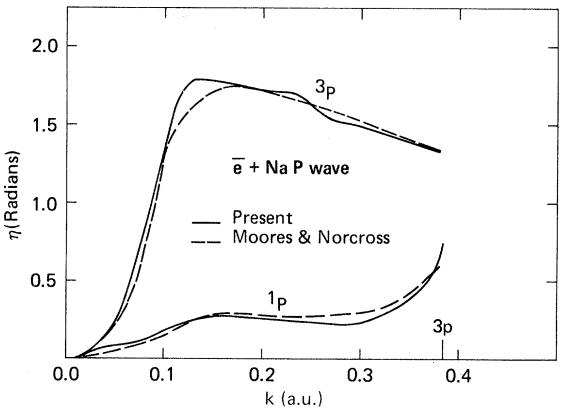


FIG. 5. $L=1$ singlet and triplet phase shifts for scattering by Na.

$k \to 0$, (b) the low-lying $^3P$ resonance, (c) the $^1P$ cusp near the first excited $3p$-state threshold, and (d) the $^1D$ resonance near the $3p$ threshold. These features can also be seen in the K results, shown in Figs. 7–9.

Close-coupling calculations on electron scattering by Li, Na, and K have also been done by Karule.[5] The present work shows good agreement with those calculations, except at thermal energies.

In regions of rapid change of the phase shifts shown in the figures, calculations were carried out on a finer grid of $k$ values than those indicated in Table I. In particular, all $^3P$ phase shifts were computed at intervals $\Delta k = 0.01$. The $^3P$ resonance in K was traced with $\Delta k = 0.001$. Small $\Delta k$ values were used for $^1P$ and $^1D$ phase shifts just below the $np$ threshold.

Some irregular structure is apparent in our results, particularly for $^3P$ phase shifts above the resonance region. Details of the variational calcula-

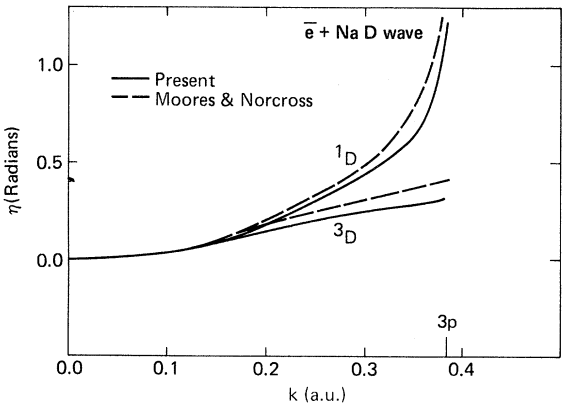


FIG. 6. $L=2$ singlet and triplet phase shifts for scattering by Na.

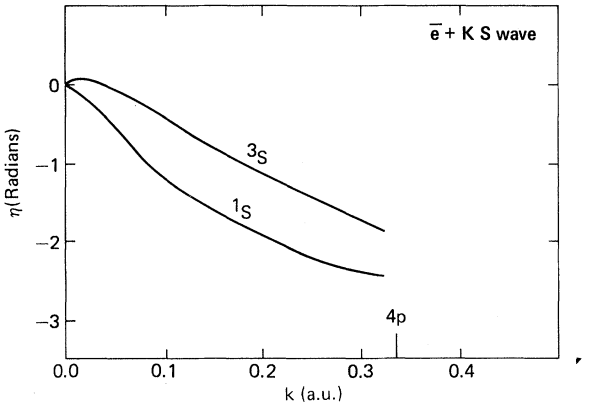


FIG. 7. $L=0$ singlet and triplet phase shifts for scattering by K.

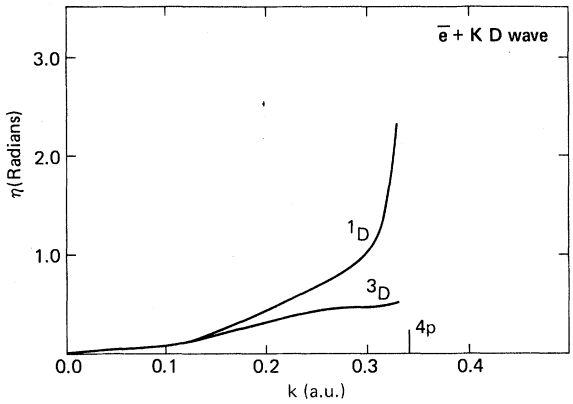


FIG. 9. $L=2$ singlet and triplet phase shifts for scattering by K.

tions (complex eigenvalues of the $m$ matrix,[4] $m'_{00}$ and $m'_{11}$ diagonal elements of similar magnitude) indicate that our results are not very close to absolute convergence of the variational expansion. This can be attributed to the strong polarization potential in alkali scattering, for which our asymptotic orbital functions are expected to be inadequate.

In the variational algorithm used here, a matrix is transformed to upper triangular form with diagonal elements ordered by increasing magnitude.[4] This ordering is achieved by a sequence of $2\times2$ rotations of the matrix, after it is reduced to triangular form by an orthogonal transformation. Computed phase shifts can have small discontinuities as functions of $k$, when diagonal elements of opposite sign cross each other in magnitude. This becomes a practical problem when the variational wave function is not well converged, as in the present work. For this reason, in calculating the $^1P$ and $^3P$ phase shifts reported here, the $2\times2$ rotation angles connecting elements of $m'_{00}$ and $m'_{11}$ were modified to interpolate smoothly between ratios of diagonal elements varying from 0.1 to 10.0.

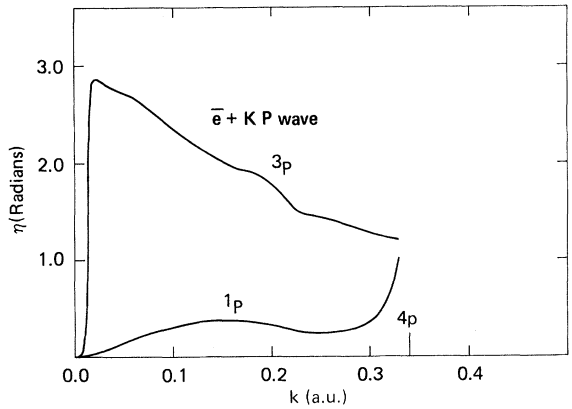


FIG. 8. $L=1$ singlet and triplet phase shifts for scattering by K.

### B. $^3P$ Resonances

The search procedure for resonances[15] has been used to locate the low-lying $^3P$ resonance just above the ground-state level of the target atom. The sets of basis functions used are given in Table I.

Our calculation gives the following values for the resonance energy $E_{res}$ and width $\Gamma$:

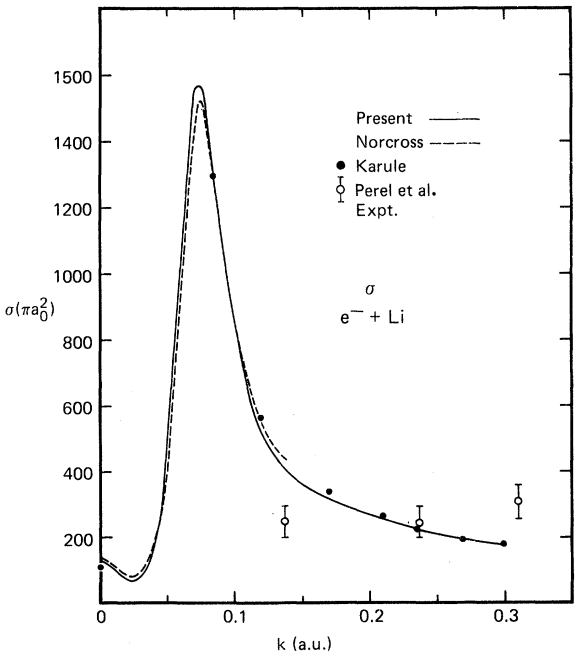


FIG. 10. Total cross section for scattering by Li.

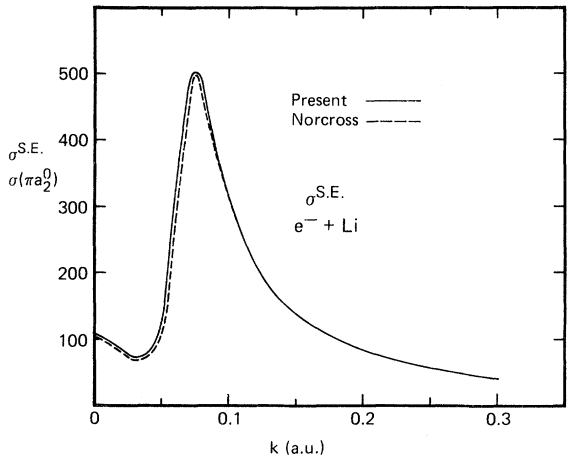


FIG. 11. Spin-exchange cross section for scattering by Li.

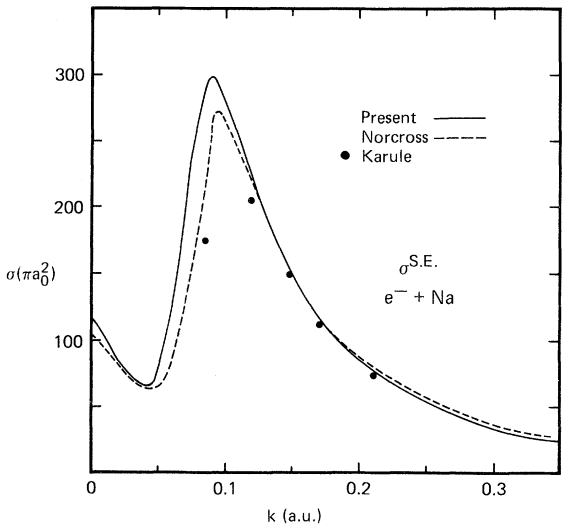


FIG. 13. Spin-exchange cross section for scattering by Na.

$Li^-$ $E_{res} = 6.0\times10^{-2}$ eV, $\Gamma = 5.7\times10^{-2}$ eV;

$Na^-$ $E_{res} = 8.3\times10^{-2}$ eV, $\Gamma = 8.5\times10^{-2}$ eV;

$K^-$ $E_{res} = 2.4\times10^{-3}$ eV, $\Gamma = 5.8\times10^{-4}$ eV.

The $^3P$ resonance is most likely caused by the strong long-range dipole potential coupling, for example, the $1s^2\,2s\,^2S$ and the $1s^2\,2p\,^2P$ states of Li. In atomic hydrogen, the $2s$ and $2p$ states are degenerate and the resulting degenerate dipole interaction causes a series of Feshbach resonances just below the $n = 2$ threshold. In the alkali atoms, no such degeneracy exists and consequently the resonance occurs above the ground-state threshold.[12]

### C. Total Cross Sections

The total scattering and spin-exchange cross sec-

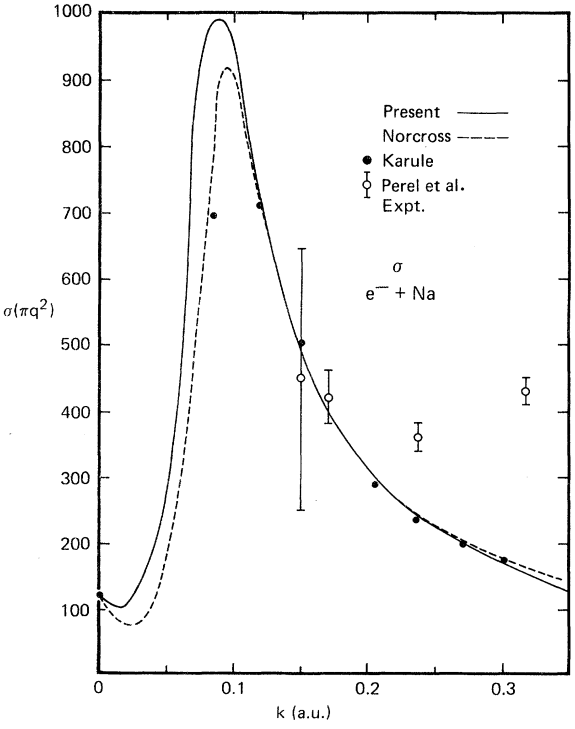


FIG. 12. Total cross section for scattering by Na.

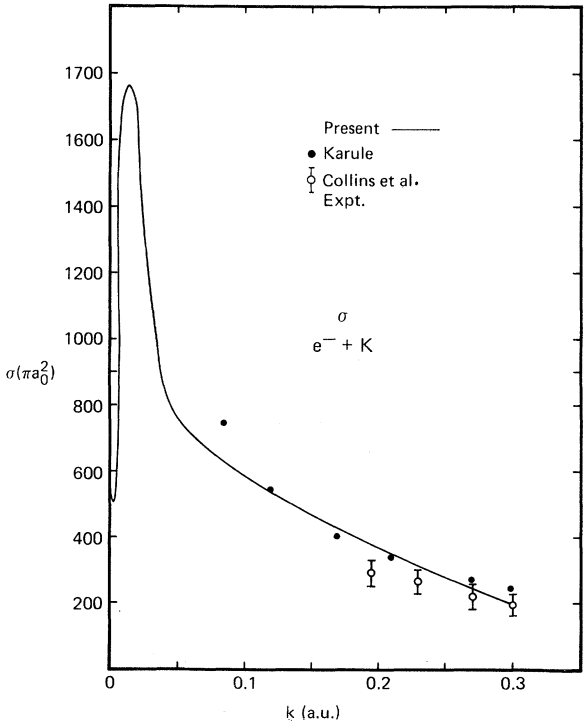


FIG. 14. Total cross section for scattering by K. The absolute measurements of Visconti *et al.* (not shown in figure) agree with those of Collins *et al.*

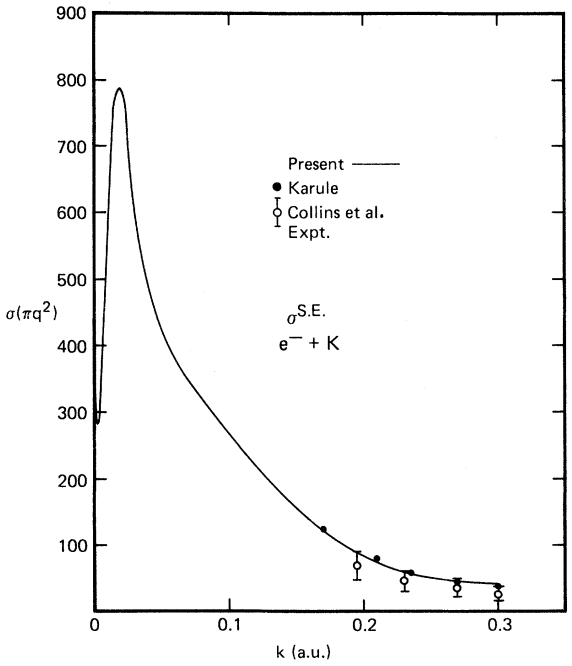


FIG. 15. Spin-exchange cross section for scattering by K.

tions are given in terms of partial cross sections

$$\sigma(k)=\sum_l [\sigma_l^+(k)+\sigma_l^-(k)] \tag{2}$$

and

$$\sigma^{se}(k)=\sum_l \sigma_l^{se}(k)\ , \tag{3}$$

where

$$\sigma_l^+(k)=\frac{\pi}{k^2}(2l+1)\sin^2\eta_l^+(k)\ ,$$

$$\sigma_l^-(k)=\frac{3\pi}{k^2}(2l+1)\sin^2\eta_l^-(k)\ , \tag{4}$$

and

$$\sigma_l^{se}(k)=\frac{\pi}{k^2}(2l+1)\sin^2[\eta_l^+(k)-\eta_l^-(k)]\ .$$

The signs (+) and (−) indicate the singlet and triplet contributions, respectively.

The total scattering and spin-exchange cross sections for scattering by Li and Na are given in Figs. 10–13. Our calculations, which include only $s$, $p$, and $d$ waves, agree well with the theoretical results of Norcross[6] and Karule.[5] There is a paucity of experimental results for the total cross sections of Li and Na. Perel *et al.*[16] give relative measurements which are normalized using the K results of Brode.[17] However, there is evidence that the absolute measurements of Brode are too large by a factor of 2 in magnitude and also in error for the energy variation.

The deviation of our total and spin-exchange cross-section curves for Na from those of Norcross,[6] shown in Figs. 12 and 13, is due to a small displacement of the position of the $^3P$ resonance. Since this resonance is associated with a virtual state of configuration $3s\,3p$, its position may be affected by a displacement of the $3p\,^2P$ threshold. With the basis orbitals indicated in Table I for $p$-wave scattering by Na, the $3p$ threshold is computed to be 2.005 eV if no virtual excitations of the $Na^+$ core are permitted. The experimental threshold is at 2.104 eV and the computed threshold, which may affect the resonance position, is low by 0.10 eV.

Since the present formalism takes into account the electronic pair correlation in configuration $n_0s\ n_0p$, this may also contribute to lowering the energy of the $^3P$ resonance.

In Figs. 14 and 15 we compare theoretical and experimental results for the total scattering and spin-exchange cross sections of K. There is good agreement between the present work, the calculation of Karule, and the absolute measurements of Collins *et al.*[18] Absolute total cross sections have also been measured by Visconti *et al.*[19] The absolute measurements of Brode are larger by a factor of 2, as mentioned above.

## IV. SUMMARY

Calculations have been made on the elastic scattering of low-energy electrons by Li, Na, and K using a variational procedure which takes polarization and correlation effects into account by means of continuum Bethe–Goldstone equations. Our phase-shift results agree well with previous calculations. There is also good agreement for the total scattering and spin-exchange cross sections with the measurements of Perel *et al.* for K. Finally, we have calculated the positions and widths of the low-lying $^3P$ resonances.

## ACKNOWLEDGMENTS

We wish to thank Dr. D. W. Norcross for very helpful correspondence and conversations. We also wish to thank Dr. R. S. Oberoi for useful discussions.

†Supported in part by the Office of Naval Research, under Contract No. N00014-72-C-0051.

*Present address: IBM, Dept. WA6, Gaithersburg, Md. 20760.

[1]A. L. Sinfailam and R. K. Nesbet, Phys. Rev. A 6, 2118 (1972); J. D. Lyons, R. K. Nesbet, C. C. Rankin, and A. C. Yates, J. Comput. Phys. (to be published).

[2]M. H. Mittleman, Phys. Rev. 147, 69 (1966); R. K. Nesbet, Phys. Rev. 156, 99 (1967).

[3]F. E. Harris and H. H. Michels, Methods Comput.

Phys. 10, 143 (1971).
[4]R. K. Nesbet and R. S. Oberoi, Phys. Rev. A 6, 1855 (1972).
[5]E. Karule, J. Phys. B 5, 2051 (1972); *Cross Sections of Electron-Atom Collisions*, edited by V. Veldre (Latvian Academy of Science, Riga, 1965), pp. 33–56 [English transl. JILA Information Center, Report No. 3, University of Colorado, Boulder, pp. 29–48 (unpublished)].
[6]D. W. Norcross, J. Phys. B 4, 1458 (1971); D. L. Moores and D. W. Norcross, J. Phys. B 5, 1482 (1972).
[7]B. Bederson, Comments At. Mol. Phys. 1, 135 (1970); Comments At. Mol. Phys. 2, 7 (1970).
[8]R. K. Nesbet, Phys. Rev. A 2, 661 (1970).
[9]E. Clementi, J. Chem. Phys. 40, 1944 (1964).
[10]E. Clementi and D. L. Raimondi, J. Chem. Phys. 38, 2686 (1963).
[11]A. W. Weiss, Astrophys. J. 138, 1262 (1963).
[12]P. G. Burke and A. J. Taylor, J. Phys. B 2, 869 (1969).
[13]P. G. Burke and H. M. Schey, Phys. Rev. 126, 163 (1962).
[14]J. N. Bardsley and R. K. Nesbet, Phys. Rev. A (to be published).
[15]R. K. Nesbet and J. D. Lyons, Phys. Rev. A 4, 1812 (1971).
[16]J. Perel, P. Englander, and B. Bederson, Phys. Rev. 128, 1148 (1962).
[17]R. B. Brode, Phys. Rev. 34, 673 (1929).
[18]R. E. Collins, B. Bederson, and M. Goldstein, Phys. Rev. A 3, 1976 (1971).
[19]P. J. Visconti, J. A. Slevin, and K. Rubin, Phys. Rev. A 3, 1310 (1971); J. A. Slevin, P. J. Visconti, and K. Rubin, Phys. Rev. A 5, 2065 (1972).

PHYSICAL REVIEW A VOLUME 7, NUMBER 6 JUNE 1973

# Coincidence Measurements of $Ar^+$-Kr Collisions at keV Energies*

R. L. Del Boca,† J. W. Montgomery, and H. C. Hayden
*Physics Department, University of Connecticut, Storrs, Connecticut 06268*
(Received 6 September 1972)

The coincidence technique of Kessel and Everhart has been used to study the $Ar^+ + Kr \rightarrow Ar^{+m} + Kr^{+n} + (m+n-1)e$ reaction at incident ion energies from 15 to 230 keV, and scattering angles from 10° to 40°, corresponding to distances of closest approach ranging from 0.38 to 0.06 Å. $\bar{Q}$ values varied from less than 100 eV to greater than 3 keV, and the average numbers of ejected electrons varied from 1/2 to 7/2 for argon and from 5/2 to 8 for krypton. Unresolved $Q$ structure is probably present at 0.2 to 0.3 Å. As with all previous data which the authors have handled where the $Q_{mn}$ profiles are not multiply peaked, the $Ar^+$-Kr $\bar{Q}$ values were found to be fit by the empirical relation $\bar{Q}_{mn} = A + BU'_m + CU''_n$ where the $U$'s are spectroscopic energy deficits, with rms errors averaging about 2.5%. Several indirect means show that the krypton is responsible for some 65% of the energy loss, possibly decreasing to about 55% at the highest $\bar{Q}_{mn}$ values studied. The intrinsic ionization probabilities from the present study reproduce fairly well the probabilities from previous $Ar^+$-Ar and $Kr^+$-Kr studies.

## I. INTRODUCTION

We used the coincidence technique of Kessel and Everhart[1] to study the

$$Ar^+ + Kr \rightarrow Ar^{+m} + Kr^{+n} + (m+n-1)e^-$$

reaction. The kinetic energies of the incident argon ions ranged from 15 to 230 keV and the scattering angles of the scattering argon ions ranged from 10° to 40°.

This paper presents the $Ar^+$-Kr experimental data and an analysis, using a method previously employed by Hayden and Knystautas,[2] to determine the inelastic energy lost by the scattered argon ion and the recoil krypton ion in the collision. The present data are compared with data from prior coincidence and noncoincidence experiments. The experimental procedure is described elsewhere[1] and is omitted here.

## II. DATA

### A. $Q$ Values

A typical inelastic-energy-loss spectrum is shown in Fig. 1, which presents data for 100 keV, 20° scattering, with all ions counted, regardless of charge state. The least-squares Gaussian curve fitted to the data has the following parameters: $\bar{Q} = 1304$ eV and $\delta Q = 575$ eV (at $1/e$ height). For the given scattering conditions, the thermal motion of the target[1] results in $\delta Q_t = 110$ eV and the instrumental broadening[1] amounts to $\delta Q_a = 450$ eV. As the broadening effects are independent and essentially Gaussian over the range of interest, the natural linewidth, calculated from $\delta Q^{N2} = \delta Q^2 - \delta Q_t^2 - \delta Q_a^2$, is 303 eV. Data of this nature, for a wide range of scattering conditions from 15 keV, 10° to 225 keV, 40° have been obtained and are presented